BG Pulse Journal USA
ISSN:1947-2536 http://www.bgpulseusa.com/index.php/bg

INTEGRATED DESIGN, OPTIMIZATION AND MECHATRONIC CONTROL OF A FOUR-SECTION ULTRASONIC AEROSOL HUMIDIFICATION SYSTEM FOR COTTON LINT BEFORE BALING

Rasul Karimovich Tadjibaev[1] · Zaylobiddin Obbosbek ugli Rakhmonov[2] Sayidmurodov Mirzohid Mirzaraximovich[3]

[1]Professor, Fergana State Technical University; [2]PhD researcher, Fergana State Technical University | Fergana, Uzbekistan ,[3]PhD in Technical Sciences, Associate Professor at Namangan State Technical University,

Doi: https://doi.org/10.5281/zenodo.24015543

Abstract: This study integrates the theoretical design, operating-regime optimization, mechatronic control and energy assessment of a four-section ultrasonic aerosol humidifier for cotton lint before baling. Fine mist is produced by piezoelectric atomization and carried in conditioned air through a moving lint layer, with flow direction alternating between consecutive sections. A sorption–transport model is linked to a three-factor Box–Behnken response analysis, while feedforward and feedback control are evaluated using a delay-based simulation. The source-reported factor–response pairs show close agreement between calculated and experimentally labelled values, and the modeled chamber substantially improves moisture uniformity relative to one-sided treatment. Air recirculation is predicted to reduce the required mist output and heating duty. The study differentiates direct source-reported observations from mathematical predictions, controller simulations and engineering estimates. The integrated findings provide a design basis for prototype validation and industrial implementation.

Keywords: cotton lint; ultrasonic atomization; cross-flow humidification; GAB–LDF model; Box–Behnken design; PLC control; air recirculation.

1. INTRODUCTION

Moisture conditioning immediately before baling affects compressibility, static charge, handling stability and the subsequent storage behavior of cotton lint. Very dry lint can become difficult to compact, while adding excessive water may increase biological activity or degrade color during storage. Accordingly, this work adopts a practical target bale-moisture range of approximately 6.5–7.5%, with particular attention to avoiding localized values above about 8–8.5% [1–4].

Conventional lint-slide spraying, steam conditioning and one-sided humid-air contact present different limitations. Liquid spray can cause wet pockets; humid steam can condense on cooler fiber; and a unidirectional air stream loses water vapor as it traverses the layer, leaving a strong thickness-wise moisture gradient. Published mill observations report modest moisture restoration with several humid-air systems [1,3]. Improving average moisture gain alone is therefore insufficient: spatial uniformity, controllability, condensation avoidance and overall utility demand must be considered together.

The present contribution combines the complementary results of four related investigations into one process-level assessment. Its core innovation is the interaction of an ultrasonic humid-air source,

stationary alternating cross-flow collectors, a time-limited sorption model and a PLC-based moisture-control strategy. The analysis focuses on internally consistent numerical and tabulated source data; it does not present newly collected production-scale measurements.

Earlier cotton-conditioning research highlights an engineering compromise between pressability and long-term fiber stability. Moisture restoration should be sufficient to reduce dry-fiber handling problems, but the maximum water content of small regions within a bale is as consequential as its mean value [1,2]. The present configuration accordingly treats cross-sectional CV and local moisture extrema as explicit design responses. This distinction becomes particularly important when the air is near saturation: a nominally acceptable average can conceal a wet inlet face and a dry outlet face.

The specific aims are to establish a consistent physical formulation, identify whether added flow-direction alternations justify extra chamber sections, retain the traceable operating-factor observations, propose a constrained working regime, and quantify the difference between atomizer electricity and the heat needed for evaporation. Each result is identified by its evidence category—analytical estimate, numerical model, source-reported tabulation or simulated controller response—so that design conclusions are not misrepresented as externally validated plant performance.

2. SYSTEM ARCHITECTURE AND ATOMIZATION PHYSICS

The proposed unit is positioned between the cotton condenser and the bale press. A mesh conveyor transfers the lint web through four fixed treatment sections. Conditioned air passes downward in Sections 1 and 3, and upward in Sections 2 and 4. Thus, a moving material element encounters three reversals without any rapidly switching damper or distributor. Upper/lower stationary collectors, sealing brushes and return filters restrict leakage and enable controlled recirculation (Fig. 1).

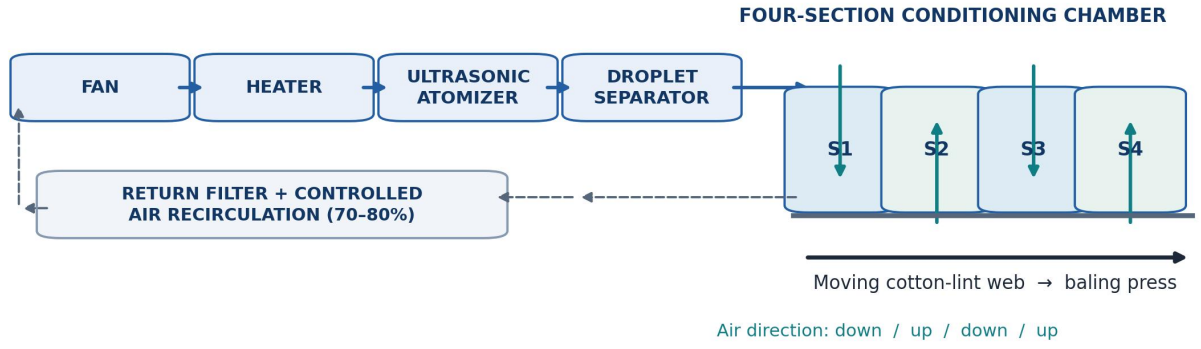


Fig. 1. Original redrawing of the proposed chamber and air-conditioning loop; arrows denote alternating air passage through successive sections.

2.1. Droplet formation and evaporation

At ultrasonic frequency f, a Lang-type capillary-wave approximation relates the characteristic droplet diameter d to the water surface tension σ and density ρw [5,6]:

$$d = 0.34\left(\frac{8\pi\sigma}{\rho_w f^2}\right)^{1/3} \quad (1)$$

Using water properties at 20 °C, the source calculation gives d ≈ 2.9 μm at 1.7 MHz and approximately 2.3 μm at 2.4 MHz. The nominal 1.7 MHz frequency was preferred for practical

transducer durability and available generator capacity. A preliminary diffusion-controlled d² law estimates evaporation [7]:

$$d^2(t) = d_0^2 - Kt, \qquad K = \frac{8D_v(\rho_{v,s} - \rho_{v,\infty})}{\rho_w} \tag{2}$$

For a nominal 3 μm droplet at 25 °C and 90% relative humidity, the source estimate is about 0.0195 s. This figure is a simplified model value, not measured device-specific mist lifetime. Close to saturation, the vapor-density driving force approaches zero; broad size distributions, coalescence, droplet cooling and wall deposition can considerably modify the real behavior. A droplet separator and independent mist balance are therefore essential.

2.2. Moist-air preparation and dew-point constraint

Atomization consumes relatively little direct electric power but subsequent evaporation requires latent heat. The humidity ratio x (kg water vapor per kg dry air) and moist-air enthalpy h (kJ per kg dry air) are calculated from standard psychrometric relationships [8]:

$$x = \frac{0.622\,\phi p_s(T)}{p - \phi p_s(T)}, \qquad h = 1.006T + x(2501 + 1.86T) \tag{3}$$

With outdoor air at 25 °C and 40% relative humidity, adiabatic conditioning to 95% relative humidity after preheating to 50 °C predicts 24.3 °C outlet air and 10.31 g/kg additional vapor. Without preheating, outlet air is estimated near 16.6 °C and moisture addition is only 3.37 g/kg. The design uses approximately 25–30 °C conditioned air at 92–95% relative humidity, subject to verification that the minimum fiber-surface temperature exceeds the local dew point. These are theoretical psychrometric states, not guaranteed operating results.

The water circuit is part of the process design rather than an ancillary utility. The dissertation calls for demineralized water, controlled bath depth (approximately 25–45 mm), water-temperature monitoring and cleaning or sterilization measures. Dissolved minerals can form fine airborne deposits after droplet evaporation, while biofilm or scale could alter output and contaminate lint. The collector geometry must also limit short-circuit airflow around the bed. Consequently, successful humidification demands coordinated water treatment, aerosol separation, air balancing and moisture measurement, not atomization in isolation.

3. COUPLED SORPTION AND CROSS-FLOW MASS TRANSFER

The lint bed is represented as a porous moving layer of surface mass ms = 1.2 kg/m². Sorption equilibrium is approximated by the Guggenheim–Anderson–de Boer (GAB) expression, with W denoting moisture on a dry-mass basis and φ the local relative humidity (fraction) [9]:

$$W_e = \frac{W_m C K \phi}{(1 - K\phi)(1 - K\phi + CK\phi)} \tag{4}$$

The illustrative parameter set is Wm = 0.042, C = 10 and K = 0.78. Since high-humidity equilibrium moisture can exceed the acceptable bale range, the exposure must be terminated during transient uptake rather than waiting for equilibrium. A linear-driving-force (LDF) law with nominal k = 0.06 s^{-1} is coupled to the quasi-steady transverse air-vapor balance [10]:

$$\frac{\partial W}{\partial t} = k(W_e - W), \qquad g\frac{\partial x}{\partial \mu} = -\frac{\partial W}{\partial t} \tag{5}$$

Here g is dry-air mass flux, μ is the lint-layer mass-depth coordinate, and x is the local air humidity ratio. Boundary conditions switch between opposite faces as material travels across successive

sections. Numerical integration uses 40 depth elements and a 0.005 s time step. The output indices are mean moisture gain and thickness-wise coefficient of variation:

$$\Delta W = \frac{1}{m_s}\int_0^{m_s} W(\mu,\tau)\,d\mu - W_0, \qquad CV = \frac{\sigma_W}{\bar{W}} \times 100\% \tag{6}$$

The wet-basis moisture used for bale control must not be confused with dry-basis sorption values. This article reports source-table gain figures in percentage points without inferring a new experimental mass basis; comparisons are made only within those source conventions.

4. STRUCTURAL SELECTION: ONE-SIDED VERSUS ALTERNATING FLOW

At an 8 s residence time, the main benefit is flattening the layer-depth profile rather than greatly increasing total uptake. Table 1 reproduces the source model outputs; the four-section arrangement retains almost the same mean gain as one-sided treatment but reduces the highest local moisture.

Air flux kg/(m²·s)	Sections	Gain (pp)	CV (%)	Local max (%)
0.30	1	1.91	12.7	8.88
0.30	2	1.87	4.6	7.43
0.30	4	1.87	4.5	7.36
0.30	8	1.87	4.5	7.33
0.45	1	2.29	11.0	8.88
0.45	2	2.25	3.4	7.59
0.45	4	2.25	3.3	7.54
0.45	8	2.25	3.3	7.51

Table 1. Model-predicted section-count effect at τ = 8 s and T = 30 °C; data from the dissertation, Table 2.7.

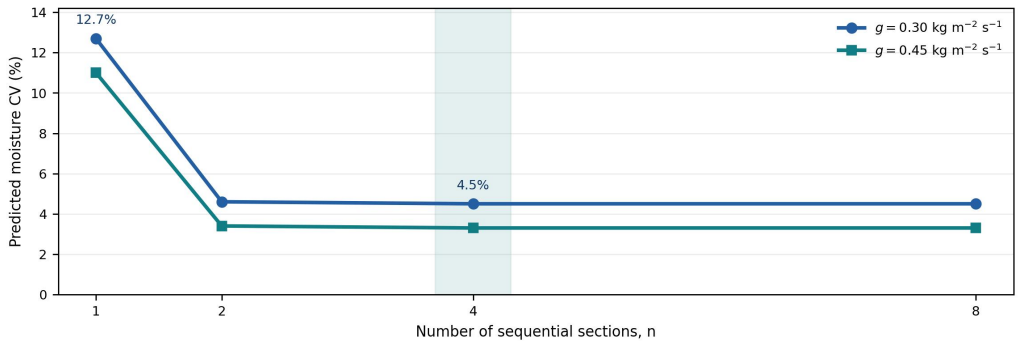


Fig. 2. Predicted thickness-wise coefficient of variation, with 4 sections selected as a design compromise.

The modeled gain in uniformity saturates by four sections (Fig. 2); eight sections offer negligible further reduction while adding ducts, seals and balancing complexity. The preferred section count is conditional on the stated bed, residence time and boundary conditions, rather than a universal optimum.

5. FACTOR–RESPONSE METHODOLOGY AND REPORTED RESULTS

A three-factor, three-level Box–Behnken design [11] was used to relate moisture gain (ΔW) and depth-wise CV to specific conditioned-air flux, lint residence time and air temperature. A single coherent design from the later dissertation matrix is retained here: X1 = (g − 0.30)/0.15; X2 = (τ − 8)/4; and X3 = (T − 30)/5. Nominal inlet relative humidity is fixed at 95%. The design consists of 12 edge points and three center-point entries. The source also contains an earlier, different factor grid; its values are not merged with Table 2.

Table 2. Three-factor Box–Behnken matrix and the source-reported calculated/experimental response pairs (ΔW in percentage points).

Run	X_1	X_2	X_3	ΔW: calc / exp (pp)	CV: calc / exp (%)
1	-1	-1	+0	0.65 / 0.67	4.2 / 4.3
2	+1	-1	+0	1.21 / 1.18	2.3 / 2.2
3	-1	+1	+0	1.77 / 1.81	8.2 / 8.4
4	+1	+1	+0	3.15 / 3.13	3.8 / 3.6
5	-1	+0	-1	0.99 / 1.02	7.6 / 7.7
6	+1	+0	-1	1.96 / 1.92	4.2 / 4.1
7	-1	+0	+1	1.51 / 1.52	5.8 / 5.8
8	+1	+0	+1	2.53 / 2.58	2.5 / 2.6
9	+0	-1	-1	0.84 / 0.82	3.5 / 3.4
10	+0	+1	-1	2.24 / 2.27	6.6 / 6.8
11	+0	-1	+1	1.15 / 1.12	2.4 / 2.3
12	+0	+1	+1	3.03 / 3.05	4.2 / 4.2
13	+0	+0	+0	1.87 / 1.85	4.5 / 4.4
14	+0	+0	+0	1.87 / 1.87	4.5 / 4.5
15	+0	+0	+0	1.87 / 1.90	4.5 / 4.6

Across the 15 tabled pairs, mean absolute differences computed from the displayed entries are 0.026 percentage points for gain and 0.10 percentage points for CV. The three center-point experimental entries provide gains of 1.85, 1.87 and 1.90 pp and corresponding CV values of 4.4%, 4.5% and 4.6%. The tight agreement within the archived matrix is informative, but independent measurement logs, calibrated sensor uncertainty and production-lot replication are not supplied.

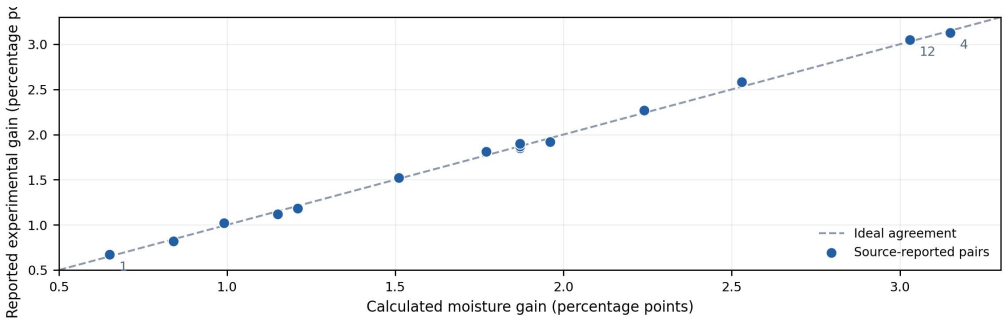


Fig. 3. Comparison of calculated and source-reported experimental moisture gains (15 regimes).

For scientific transparency, the "experimental" designation follows the source tables. The original record specifies oven-drying and moisture measurements, but gives inconsistent drying temperatures across subsections and does not provide the raw replicate archive or an independently auditable ANOVA. This study therefore does not infer missing uncertainty intervals or new experimental confirmation.

6. RESPONSE SURFACE AND CONSTRAINED OPERATING POINT

The dissertation approximates calculated responses with the following second-order polynomials. All X variables are coded as defined above; the displayed terms are preserved exactly from the source without inventing unreported coefficients:

$$\Delta W = 1.866 + 0.490X_1 + 0.793X_2 + 0.274X_3 + 0.208X_1X_2 + 0.118X_2X_3 - 0.120X_1^2 - 0.051X_2^2 \quad (7)$$

$$CV = 4.53 - 1.614X_1 + 1.303X_2 - 0.888X_3 - 0.630X_1X_2 - 0.338X_2X_3 + 0.463X_1^2 - 0.366X_2^2 \quad (8)$$

The largest positive linear contribution to gain is residence time (X2), followed by air flux (X1); increasing air flux has the largest negative coefficient in the CV model. The positive X2 coefficient in CV reflects that prolonged exposure can widen depth-wise differences unless adequate flow is maintained. The rational point was selected by constraining mean moisture to approximately 7.0 ± 0.3%, CV and maximum local moisture rather than maximizing ΔW alone. For lint entering at roughly 4.5%, the reported model-based selection is g = 0.45 kg/(m²·s), τ = 10 s, T = 30 °C and φ = 95%, giving ΔW ≈ 2.7 pp, CV ≈ 3.6% and Wmax ≈ 8.1%. These point estimates require direct testing.

7. PLC-BASED FEEDFORWARD AND FEEDBACK REGULATION

The mechatronic design coordinates generator-module output, heater power, fan speed and conveyor speed. Sensor S1 measures incoming lint moisture and supports mass-balance feedforward correction; S2 measures conditioned lint for fast feedback; S3 provides supervisory bale-moisture monitoring. Set-point limitation, water-level sensing, airflow-loss interlocks and protection against over-heating are integrated at PLC level in accordance with the proposed architecture (Fig. 4) [12,13].

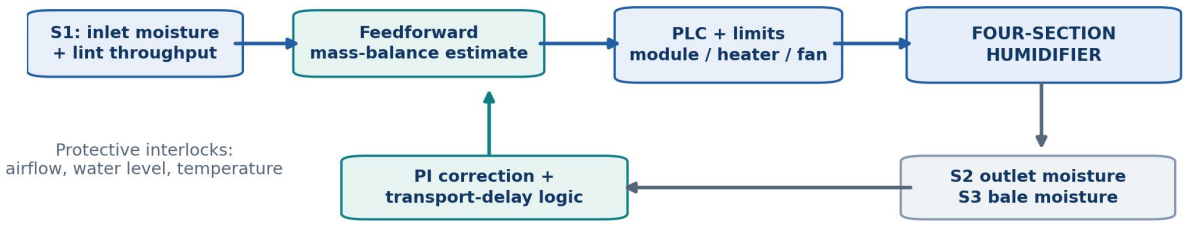


Fig. 4. Reconstructed feedforward–feedback control structure with bale supervision and protective interlocks.

For preliminary tuning, the moisture-control process is approximated by a first-order-plus-dead-time (FOPDT) model [14]. The parameters K = 3.5 percentage points, Tp = 20 s and θ = 150 s are simulation assumptions, not parameters identified from an operating production line:

$$G(s)=\frac{Ke^{-\theta s}}{T_p s+1}, \qquad u=\mathrm{sat}(u_{ff}+u_{PI}), \qquad u_{ff}(t)=\frac{W^{*}-W_0(t-t_d)}{K} \tag{9}$$

After a simulated inlet-moisture decrease from 4.5% to 3.8% with a 7.0% set point, the source model compares the following controller alternatives. The integrated absolute error (IAE) is expressed in %·min.

Control strategy	Minimum bale moisture (%)	Maximum bale moisture (%)	IAE (%·min)
Constant atomizer output	6.30	7.00	32.90
PI feedback alone	6.30	7.03	3.79
Feedforward + PI feedback	6.64	7.32	0.25

The combined scheme stays within the targeted 6.5–7.5% band in this specific simulated disturbance. It reduces simulated IAE by about a factor of 15 relative to PI alone; real gains depend on sensor precision, material delay and controller commissioning.

A production implementation would also require synchronizing S1 measurements with the same fiber mass when it reaches the treatment chamber, filtering noisy signals, enforcing output saturation with integral anti-windup, and specifying safe operating modes when the condenser or bale press stops. The reported 150 s downstream delay reinforces the role of the inlet-moisture feedforward channel; a feedback-only controller cannot respond before the delayed product reaches S3. Controller settings should be re-identified after installation rather than copied from the illustrative model.

8. INDUSTRIAL SIZING AND SYSTEM-LEVEL ENERGY ASSESSMENT

For a 2.5 t/h lint-processing line, the preliminary design adopts a 1.85 m by 2.50 m working chamber with four sections of 0.625 m each. The relevant sizing relationship uses surface lint loading ms and residence time τ (equation 10). At g = 0.30 kg/(m²·s) and τ = 8 s, the calculated treatment area is 4.63 m² and the nominal air supply approximately 4,300 m³/h. These geometric design conditions are distinct from the subsequently selected 10 s response-surface operating point.

$$A = \frac{G\tau}{3600 m_s}, \qquad Q_a = gA, \qquad T_k = \frac{\tau}{n} \tag{10}$$

Table 3. Source-derived nominal sizing of the proposed industrial humidifier.

Component / parameter	Preliminary engineering specification
Aerosol generator	1.7 MHz; 20 modules; 200 transducers (16 duty + 4 reserve)
Mist output and atomizer electricity	~54–56 kg/h duty; ≤70 kg/h maximum; 4.8–6.0 kW
Air supply and pressure loss	~4,300 m³/h; total calculated resistance 847 Pa
Mechanical drives	Fan motor 2.2 kW; conveyor gear motor 0.37 kW
Humid-air regime	25–30 °C; 92–95% relative humidity
Thermal preparation	~40–45 kW heater duty under 70–80% recirculation

The return-air fraction influences generator duty as well as the heat necessary to establish the target air state. Table 4 and Fig. 5 reproduce source energy-balance predictions for ambient air at 25 °C and 40% relative humidity; they are not measured plant consumption.

Table 4. Calculated air-recirculation trade-off at 2.5 t/h lint throughput.

Recirculation (%)	Mist duty (kg/h)	Heater (kW)	Atomizer electric (kW)
0	89.3	70.5	8.0
50	67.5	51.5	6.1
70	58.8	43.9	5.3
80	54.4	40.0	4.9

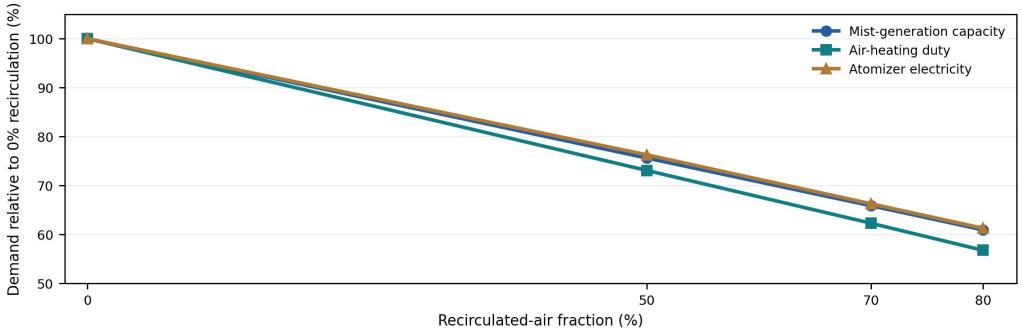


Fig. 5. Normalized source-estimated generator and heating demands as the fraction of air returned increases.

At 80% recirculation, the model predicts 39% less mist demand and 43% less heater duty than with 100% fresh air. For a nominal 55 kg/h water output, a conventional electric steam generator is

estimated to require 41.3 kW of electricity, versus 4.9 kW direct electricity for the ultrasonic generator. However, the ultrasonic system also requires about 40 kW of thermal power for air preparation. The device does not eliminate evaporation energy; its potential is to use recoverable or lower-cost heat, with attention to fan electricity, filtration and dew-point management.

At the stated 4,000-hour seasonal operating assumption, these loads can be translated into indicative utility expenditures, but the answer changes with the purchased-heat and electricity tariffs. The dissertation also offers a capital-cost and payback scenario, which is not treated here as a verified financial result because the facility-specific operating history and product-quality benefits have not been independently documented. A robust comparison should use separate meters for heater thermal delivery, generator electricity, fan power and conveyor drive, together with actual water uptake and rejected condensate.

9. DISCUSSION, UNCERTAINTY AND VALIDATION PRIORITIES

The four contributions form a coherent but still validation-dependent technology proposition. The capillary-wave and evaporation models justify fine-mist generation; the GAB–LDF air/lint model explains why alternating the air-entry face reduces a depth gradient; the Box–Behnken matrix supplies a bounded operating window; and the PLC concept responds to variability in incoming lint and process delay. Together these elements target moisture quality—adequate average gain without a locally excessive wet fraction—rather than simply increased water addition.

Several limits must be explicitly retained. First, droplet lifetime estimates neglect detailed heat exchange, size spectra and deposition. Second, the sorption constants and LDF rate were adopted as engineering inputs rather than calibrated for a variety-specific lint lot. Third, the two source factor grids, inconsistent oven-temperature descriptions and absent full raw measurement files constrain reproducibility. Fourth, the controller time constant and transport delay are simulation assumptions. Fifth, economic and thermal assessments depend on utility tariffs, available waste heat, filter fouling and actual circulation losses. The apparent economy of atomizer electricity must never be mistaken for equivalently lower total energy input.

A rigorous next test should measure droplet-size distributions, generator output, captured condensate and wall deposits; compare layer moisture at the top, center and bottom under matched throughput for one-sided and alternating chambers; determine true belt-air pressure losses; calibrate inlet, outlet and bale sensors against one specified oven-drying method [15]; and record both kWh and delivered thermal energy. Replicated lint-quality and bale-storage evaluations would establish whether the simulated improvements persist under industrial conditions.

10. CONCLUSIONS

An integrated four-section, valve-free ultrasonic humidification design is formulated for lint conditioning before baling. Within the reported model, alternating flow reduces CV from 12.7% to 4.5% at $g = 0.30$ kg/(m²·s), $\tau = 8$ s, while nearly preserving the modeled moisture gain. The coherent 15-point response matrix supports a calculated rational operating condition of $g = 0.45$ kg/(m²·s), $\tau = 10$ s and $T = 30$ °C. A feedforward–PI control simulation improves the disturbance response, while 70–80% air recirculation reduces estimated mist and heater demand. These are differentiated as design predictions, source-reported observations and simulation outputs—not independent industrial validation.

Data provenance

Tables 1–4 and the plotted data are synthesized from the provided manuscripts and dissertation. The figures are original redrawings of the cited numerical findings; no missing raw measurements, confidence intervals or industrial trials were fabricated.

REFERENCES

1. Gordon, S., Horne, S., van der Sluijs, R. (2007). Moisture in cotton ginning review: Final report, CRDC Project CTFT20. Cotton Research and Development Corporation.
2. Chun, D.T.W., Anthony, W.S. (2004). Effects of adding moisture at the gin lint slide on cotton bale microbial activity and fiber quality. Journal of Cotton Science, 8, 83–90.
3. Rutherford, R.D. et al. (2013). Field evaluation of the Lummus bale moisture monitor. Proceedings of the Beltwide Cotton Conferences, 1215–1220.
4. Montalvo, J.G., Von Hoven, T.M. (2008). Review of standard test methods for moisture in lint cotton. Journal of Cotton Science, 12, 33–47.
5. Lang, R.J. (1962). Ultrasonic atomization of liquids. Journal of the Acoustical Society of America, 34(1), 6–8.
6. Rajan, R., Pandit, A.B. (2001). Correlations to predict droplet size in ultrasonic atomisation. Ultrasonics, 39(4), 235–255.
7. Hinds, W.C. (1999). Aerosol Technology: Properties, Behavior, and Measurement of Airborne Particles, 2nd ed. Wiley.
8. ASHRAE (2017). Handbook—Fundamentals, Chapter 1: Psychrometrics. ASHRAE.
9. Timmermann, E.O. (2003). Multilayer sorption parameters: BET or GAB values? Colloids and Surfaces A, 220, 235–260.
10. Crank, J. (1975). The Mathematics of Diffusion, 2nd ed. Clarendon Press.
11. Box, G.E.P., Behnken, D.W. (1960). Some new three level designs for the study of quantitative variables. Technometrics, 2(4), 455–475.
12. IEC (2013). IEC 61131-3: Programmable controllers—Part 3: Programming languages.
13. Åström, K.J., Hägglund, T. (2006). Advanced PID Control. ISA.
14. Skogestad, S. (2003). Simple analytic rules for model reduction and PID controller tuning. Journal of Process Control, 13(4), 291–309.
15. ASTM International. ASTM D2495: Standard Test Method for Moisture in Cotton by Oven-Drying.